General Disclaimer

One or more of the Following Statements may affect this Document

- This document has been reproduced from the best copy furnished by the organizational source. It is being released in the interest of making available as much information as possible.

- This document may contain data, which exceeds the sheet parameters. It was furnished in this condition by the organizational source and is the best copy available.

- This document may contain tone-on-tone or color graphs, charts and/or pictures, which have been reproduced in black and white.

- This document is paginated as submitted by the original source.

- Portions of this document are not fully legible due to the historical nature of some of the material. However, it is the best reproduction available from the original submission.

NASA Technical Memorandum 83466

Study of a LH_2-Fueled Topping Cycle Engine for Aircraft Propulsion

George E. Turney and Laurence H. Fishbach
Lewis Research Center
Cleveland, Ohio

Prepared for the
Aircraft Design Systems and Operations Meeting
cosponsored by the AIAA and AHS
Fort Worth, Texas, October 17-19, 1983

NASA

STUDY OF A LH_2-FUELED TOPPING CYCLE ENGINE FOR AIRCRAFT PROPULSION

By
George E. Tuiney and Laurence H. Fishbach

National Aeronautics and Space Administration
Lewis Research Center
Cleveland, Ohio 44135

Abstract

An analytical investigation was made of a topping cycle aircraft engine system which uses a cryogenic fuel. This system consists of a main turboshaft engine which is mechanically coupled (by cross-shafting) to a topping loop which augments the shaft power output of the system.

The thermodynamic performance of the topping cycle engine was analyzed and compared with that of a reference (conventional-type) turboshaft engine. For the cycle operating conditions selected, the performance of the topping cycle engine in terms of brake specific fuel consumption (bsfc) was determined to be about 12 percent better than that of the reference turboshaft engine.

Engine weights were estimated for both the topping cycle engine and the reference turboshaft engine. These estimates were based on a common shaft power output for each engine. Results indicate that the weight of the topping cycle engine is comparable to that of the reference turboshaft engine.

E-1735

Nomenclature

bsfc	brake specific fuel consumption, $\frac{lb_{fuel}}{hp\text{-}hr}$
$C_{p,a}$	specific heat of air at constant pressure, $\frac{Btu}{lb_m - °R}$
ϵ	turbomachine efficiency
H	enthalpy, $\frac{Btu}{lb_m}$
ΔH_{comb}	heat of combustion of hydrogen fuel, 51500 $\frac{Btu}{lb_m}$
H_i	enthalpy of component i in gas mixture, $\frac{Btu}{lb_m}$
H_{mix}	enthalpy of gas mixture (equation (7)), $\frac{Btu}{lb_m}$
K	conversion factor (equations (4) and (6)), 3.927×10^{-4} $\frac{hp - hr}{Btu}$
Ma	Mach number
P	total pressure, psia
Q_{HX-1}	heat transfer rate in heat exchanger HX-1, $\frac{Btu}{hr}$
Q_{HX-2}	heat transfer rate in heat exchanger HX-2, $\frac{Btu}{hr}$
S	entropy, $\frac{Btu}{°R}$
SP	shaft power output of engine, horsepower (hp)
T	temperature, °R
W_a	air flow rate, $\frac{lb_m}{hr}$
W_{bleed}	bleed air flow rate, $\frac{lb_m}{hr}$
W_f	fuel flow rate, $\frac{lb_m}{hr}$
W_i	flow rate of component i in flow mixture (equation (7)), $\frac{lb_m}{hr}$
γ	specific heat ratio for air
η	thermal efficiency
X	fraction of total fuel which is burned in burner B2

Subscripts:

0	refers to atmospheric free-stream conditions
1, 2,..., 19	flow station designations (see Figs. 3 and 4)
id	ideal
j	refers to flow station j
j-1	refers to flow station j-1

Introduction

The problem of meeting the nation's energy needs in the coming years has become a subject of increasing concern. The escallating worldwide demand for energy is now causing an accelerated depletion of some of the world's key energy resources. In the foreseeable future, this problem could become acute for some resources,

particularly petroleum - which is the basic resource for production of all aviation fuels.

Figure 1 (constructed from published data[1]) shows projected depletion trends in petroleum resources for three different annual consumption growth rates. It is apparent from this figure that the world's oil resources are limited and could be depleted in a relatively short period of time. When crude oil production rates are considered, it appears that supply shortages could develop long before the crude oil reserves are depleted. For instance, Fig. 2 shows an estimate of the maximum production rate of crude oil in future years. The maximum production rate shown here was obtained from published estimates[1] and represents the maximum rate at which crude oil can be supplied to the consumer market. At a zero-demand growth rate, Fig. 2 indicates that shortages may develop in about 32 years. And with a 2 percent growth rate, shortages may be felt in about 15 years.

The depletion of crude oil resources has prompted the NASA and others to investigate alternate energy resources for the production of aviation fuels. Studies conducted by NASA[2] have concluded that liquid hydrogen (LH_2), liquid methane (LCH_4) and synthetic aviation kerosene (or synjet) are the three most promising alternate fuels for aviation. All of these fuels can be produced synthetically from coal - one of our most abundant fossil fuel resources.

Liquid hydrogen (LH_2) and liquid methane (LCH_4) are cryogenic fuels which have been studied extensively for both subsonic and supersonic transport aircraft[3,4]. The advantages and disadvantages associated with the use of cryogenic fuels for transport aircraft are well known. Storage and handling are considered to be a prime drawback. But the cryogenic state of these fuels can be used advantageously to improve the performance of aircraft propulsion systems. For example, cryogenic fuels can be used effectively as a heat sink to reduce or eliminate the need of compressor bleed air for turbine cooling. Other schemes for improving engine performance have been investigated[5]. They include: using cryogenic fuel as a heat sink to precool the compressor airflow, expanding heated fuel through an auxiliary turbine to produce additional shaft work and preheating a portion of the fuel before burning in a combustor.

In this report, a topping cycle gas turbine engine is introduced which uses cryogenic fuel and which combines all of the above mentioned schemes for augmenting engine performance. This engine (hereafter referred to as the "topping cycle engine") consists of a main turboshaft engine which is augmented by a direct-coupled secondary power generation loop (or topping loop). The topping loop operates with precooled compressor air and a fuel-rich combustor. The fuel-rich combustion products are expanded through an auxiliary turbine in this loop and are then fed into the burner of the main turboshaft engine where the excess fuel is burned completely

The study presented in this report deals primarily with the thermodynamic performance characteristics of this engine system. As a part of this study, assessments were also made of the weight associated with this engine system. Results of the thermodynamic analysis and the engine weight analysis are described in this report.

This engine study is based on the use of liquid hydrogen fuel. However, in principle, the topping cycle engine could operate with other cryogenic fuels, such as liquid methane.

Description of Topping Cycle Engine

As an aid in explaining the topping cycle engine, consider first a simplified version of a hydrogen fueled turboshaft engine such as shown in Fig. 3. Air entering this engine is compressed by the compressor (C1) and is then mixed with the hydrogen fuel pumped from the storage tank. The mixture is burned and the combustion products are expanded through the turbine to produce work. The work produced by the turbine drives the main compressor and fuel pump and also powers an external load. The external load in this system could be a fan, a propeller or some other propulsive component.

Figure 4 shows the same turboshaft engine with a topping loop added. In this system, a fraction of the compressor airflow from the main engine is bled off at an interstage point and fed to the topping loop. The topping loop in this system operates as an auxiliary power unit. The bleed air entering this loop is precooled and compressed in two separate processes. Precooling is accomplished with hydrogen-to-air heat exchangers as shown in Fig. 4. Precooling is advantageous in that it lowers the air temperature ahead of the compressors thereby reducing the compression work.

The total engine fuel flow is fed directly into the topping loop burner. The topping loop burner operates highly fuel-rich with an equivalence ratio (ER) ranging somewhere between about 2.5 and 4.5. The equivalence ratio is defined as follows:

$$ER = \frac{\text{Actual fuel-to-air ratio}}{\text{Stoichiometric fuel-to-air ratio}}$$

Thus, only a fraction of the total fuel flow is burned in the topping loop.

The combustion products from the topping loop include hydrogen - the unburned fuel, nitrogen and water vapor. (All oxygen is consumed in the fuel-rich burning process.) The fuel-rich combustion products are expanded through the topping loop turbine and ducted directly into the main engine burner. There, the fuel mixture is combined with the remaining air from the main engine, burned completely and expanded through the main engine turbine. Typically, the main engine burner operates at an equivalence ratio (ER) ranging from about 0.2 to 0.5.

As indicated in Fig. 4, the topping loop and the main turboshaft engine are interconnected by a cross-shaft so that power produced by the topping loop turbine is supplied to the compressors and to the main engine load. Thus, the topping loop operates as an auxiliary powerplant and produces additional power which is transferred to the system load. The performance benefits of this cycle

are described in the Results section of this report.

Analytical Approach

The primary purpose of this study was to evaluate and assess the thermodynamic performance of the topping cycle engine. But, in addition to the thermodynamic or cycle analysis, engine component and system weights were also evaluated.

As a first step in the approach to this study, a reference or "baseline" engine was established to serve as a standard by which the topping cycle engine could be compared. The baseline engine is the hydrogen fueled turboshaft engine depicted in Fig. 3 and described in the preceding section.

For the thermodynamic analysis, analytical models representing both the baseline engine (Fig. 3) and the topping cycle engine (Fig. 4) were developed. All engine performance calculations for this study were based on cruise flight conditions at Mach 0.80, 35,000 feet altitude.

To systematically evaluate the thermodynamic performance of the topping cycle engine, appropriate equations were developed for both the topping cycle and baseline engines. Digital codes were then formulated for calculating the performance characteristics of these engines. Fluid thermodynamic properties for the analysis were taken from three sources: Properties for parahydrogen, nitrogen and oxygen were taken from Hendricks et. al[6]. And properties for air and steam were obtained from Fishbach[7] and Hendricks et. al[8].

For the purpose of estimating engine system weights, a digital computer code, called WATE-2[9], was used. This program is capable of estimating weights and dimensions of individual components (such as compressors, turbines, burners, etc.) as well as total engine system weights. The WATE-2 program was used in this study to estimate weights of both the baseline engine and the topping cycle engine. A reference shaft power output of 10,000 horsepower was assumed as a basis for estimating and comparing the weights of these engine systems.

The analytical procedure along with the assumptions and equations used in this study are described in the following paragraphs.

Thermodynamic Analysis

Cycle Conditions and Component Characteristics. Cycle operating conditions and component characteristics were established for the purpose of providing a consistent set of reference conditions for use in computing and comparing the performance of the baseline engine and topping cycle engine. Table I is a listing of the assumed cycle operating conditions (design point conditions) and the component characteristics. As indicated in this table, all components which are common to both of these engines (such as inlets, compressors, burners and turbines) have identical characteristic values. The component efficiencies listed in Table 1 are considered to be representative of current day aircraft engine technology.

Figure 5 is a temperature-entropy diagram for the topping cycle engine operating at the assumed design point conditions of Table 1. This figure shows the pressures and temperatures at each of the major points throughout this engine. As indicated in Fig. 5, both burners in this engine system operate at a design point temperature level of 3000° R. This temperature level is considered to be representative of an advanced technology engine.

The bleed air entering the topping loop is taken from an interstage point of compressor C1. The pressure of the bleed air was assumed to have a design value of of 81.0 psia. This pressure level was chosen to provide nearly-equal heat transfer rates in the individual heat exchangers of the topping loop.

In the analysis of this engine system, a pressure matching constraint was imposed such that the exhaust stream pressure from turbine T2 was equal to the stream pressure in the main engine burner B1.

Cycle Analysis. Normally, in cycle analyses, the conventional index used in rating the performance of aircraft propulsion systems is the "specific fuel consumption". For turboshaft engines, such as the baseline engine and the topping cycle engine, the brake specific fuel consumption, bsfc, is used and is defined as:

$$bsfc = \frac{\text{Fuel flow rate}}{\text{Net shaft power delivered to load}} = \frac{W_f}{SP} \quad (1)$$

Another index used to indicate aircraft propulsion system performance is the thermal efficiency. The thermal efficiency, η, is directly related to the bsfc. For turboshaft engines, the thermal efficiency is defined as:

$$\eta = \frac{\text{Net shaft power delivered to load}}{\text{Chemical energy input}}$$

$$= \frac{SP}{K\,(W_f)(\Delta H_{comb})} \quad (2)$$

In equations (1) and (2), the net shaft power delivered to the load, SP, represents the total turbine power developed less the power absorbed by the compressor(s) and pump. For the baseline engine (Fig. 3), the net shaft power delivered to the load is:

$$\begin{matrix}\text{Baseline} \\ \text{engine} \\ SP\end{matrix} = \begin{matrix}\text{Power developed} \\ \text{by} \\ \text{turbine T1}\end{matrix} - \begin{matrix}\text{Power consumed} \\ \text{by} \\ \text{compressor C1}\end{matrix} - \begin{matrix}\text{Power consumed} \\ \text{by} \\ \text{pump P}\end{matrix} \quad (3)$$

Or, in terms of the respective flow rates and enthalpies, equation (3) becomes:

$$\begin{matrix}\text{Baseline} \\ \text{engine} \\ SP\end{matrix} = K[(W_a + W_f)(H_4 - H_5) - W_a(H_2 - H_1) - W_f(H_7 - H_6)] \quad (4)$$

And for the topping cycle engine (Fig. 4), the net shaft power delivered to the load is:

$$\begin{aligned}\text{Topping cycle engine SP} = {} & \text{Power developed by turbine T1} + \text{Power developed by turbine T2} \\ & - \text{Power consumed by compressor C1} - \text{Power consumed by compressor C2} \\ & - \text{Power consumed by compressor C3} - \text{Power consumed by pump P}\end{aligned} \tag{5}$$

Expressed in terms of the respective flow rates and enthalpies, equation (5) becomes:

$$\begin{aligned}\text{Topping cycle engine SP} = {} & K\,[(W_a + W_f)(H_4 - H_5) + (W_{bleed} + W_f) \\ & \times (H_{14} - H_{15}) - (W_a - W_{bleed})(H_2 - H_1) \\ & - W_{bleed}(H_8 - H_1) - W_{bleed}(H_{10} - H_9) \\ & - W_{bleed}(H_{12} - H_{11}) - W_f (H_7 - H_6)]\end{aligned} \tag{6}$$

Some of the enthalpy terms in equations (4) and (6) represent a weighted average for two or more component fluids. For example, the enthalpy at flow station numbers 14 (i.e., H_{14}) is the average enthalpy per pound of fluid mixture containing nitrogen, hydrogen, and water vapor. The enthalpy of the mixture is dependent upon the composition of the flow mixture. An appropriate expression was used to compute the enthalpy per unit mass of flow mixture. In equation form, the enthalpy of a unit mass of fluid consisting of a mixture of n component gases is:

$$H_{mix} = \frac{\sum_{i=1}^{i=n} (W_i H_i)}{\sum_{i=1}^{i=n} W_i} \tag{7}$$

Engine Component Analysis. In order to solve equations (4) and (6), the respective enthalpies in these equations must be determined. Starting at the engine inlet, the enthalpy terms were evaluated from thermodynamic relationships applied to the specific components in these systems. Pressures at the inlet and outlet of each component were determined from the design point pressures and pressure ratios listed in Table I. The equations and procedure applied to the specific components in the engine systems are presented in the paragraphs which follow.

(1) Engine inlet - Beginning with free-stream conditions at 35,000 feet altitude and assuming an inlet recovery of 1.0 as stated in Table I, the total pressure and total temperature at the inlet (station 1) were computed as follows:

$$P_1 = P_0 \left(1 + \frac{\gamma - 1}{2} Ma^2\right)^{\gamma/\gamma-1} \tag{8}$$

$$T_1 = T_0 \left(1 + \frac{\gamma - 1}{2} Ma^2\right) \tag{9}$$

The enthalpy and entropy of air at station 1 were then obtained from an air properties subroutine formulated from data in NNEP[7]. In functional notation, the enthalpy and entropy relationships are as follows:

$$H_1 = f(P_1, T_1) \tag{10}$$

and

$$S_1 = f(P_1, T_1) \tag{11}$$

(2) Turbomachinery - The fluid conditions at the outlet of a turbomachinery component (such as a compressor, turbine, or pump) were determined as described below.

Designating the outlet and inlet flow stations as "j" and "j-1", respectively, the outlet fluid conditions were computed as follows. For a constant entropy process, the ideal enthalpy at station j ($H_{j,id}$) is given by:

$$H_{j,id} = f(P_j, S_{j-1}) \tag{12}$$

For the compressors and pump, the actual enthalpy at flow station j is:

$$H_j = H_{j-1} + \frac{(H_{j,id} - H_{j-1})}{\epsilon} \tag{13}$$

And for the turbines, the actual enthalpy at station j is:

$$H_j = H_{j-1} + \epsilon(H_{j,id} - H_{j-1}) \tag{14}$$

Fluid temperatures (corresponding to the actual enthalpies and pressures at station j) were then obtained directly from a subroutine of fluid properties.

(3) Burners - The stoichiometric fuel-to-air mass ratio with hydrogen fuel is .029152. In order to limit the burner outlet temperature to a reasonable preset value, the engine burners must be operated either fuel-rich (ER > 1.0) or air-rich (ER < 1.0). As stated in the section Description Of Topping Cycle Engine, the topping loop burner (B2) operates fuel-rich; and the main engine burner (B1) operates air-rich.

The rate of heat release in the respective burners is directly proportional to the rate at which fuel is reacted.

(a) Baseline engine - In the baseline engine (Fig. 1), all fuel entering the main burner (B1) is reacted with excess air. And the rate of heat release is given by:

$$\text{Rate of heat release in burner B1} = W_f \Delta H_{comb} \tag{15}$$

The mass ratio of fuel flow to total air flow, $\frac{W_f}{W_a}$, required to achieve a specified

value of burner outlet temperature, T_4, is obtained from the heat balance equation. That is,

$$W_f \, \Delta H_{comb} = (W_a + W_f)(H_4 - H_3) \tag{16}$$

Rearranging equation (16) and solving for the fuel-to-air mass flow ratio gives:

$$\frac{W_f}{W_a} = \frac{(H_4 - H_3)}{\Delta H_{comb} - (H_4 - H_3)} \tag{17}$$

The enthalpies of the flow mixtures, i.e., H_3 and H_4, were calculated from the relationship given by equation (7). The value of H_4 in equation (17) is dependent on the temperature and pressure at flow station 4 and also on the fuel-to-air mass flow ratio. Thus, an iterative procedure was used to solve equation (17) for the fuel-to-air mass flow ratio.

(b) Topping cycle engine - In the topping cycle engine (Fig. 4), burner B2 operates fuel-rich and the main burner, B1, operates air-rich. Representing the fuel fraction burned in burner B2 by X, the rate of heat release in burner B2 is given by the equation

$$\text{Rate of heat release in burner B2} = X(W_f)(\Delta H_{comb}) \tag{18}$$

The products of combustion from burner B2 consist of water vapor, nitrogen and hydrogen - the unburned fuel. (All oxygen supplied with the bleed air entering B2 is reacted.) The mixed-mean temperature out of burner B2, i.e., T_{14} of Fig. 4, is specified (see Table I) and has a design point value of 3000° R. By rearrangement of the heat balance equation for burner B2, we obtained the following expression for the mass fraction of total fuel flow which is burned in this burner.

$$X = \frac{\left(1 + \frac{W_{bleed}}{W_f}\right)(H_{14} - H_{13})}{\Delta H_{comb}} \tag{19}$$

An iterative procedure was used to solve equation (19). The first step in the procedure was to assume a value for the fuel-to-bleed air mass flow ratio, $\frac{W_f}{W_{bleed}}$. Then, since all oxygen present in the bleed air entering burner B2 is consumed, we independently computed a value for X from a mass balance around this burner. Using the initial values of $\frac{W_f}{W_{bleed}}$ and X, we then calculated the composition of the combustion products leaving burner B2. The enthalpy of the combustion product mixture, H_{14}, was then calculated from equation (7) for a preselected design point temperature of 3000° R. This procedure was repeated, as required, until a solution of equation (19) was obtained.

The fuel-rich combustion products from burner B2 are expanded through the topping loop turbine and fed directly into the main engine burner (B1). There, the excess fuel in the mixture is combined with the remaining air from the main engine and burned completely. The mass flow rate of fuel entering the main burner (B1) is equal to $(1 - X)\, W_f$. And the rate of heat release in burner B1 is given by the following equation.

$$\text{Rate of heat release in burner B1} = (1 - X)(W_f)(\Delta H_{comb}) \tag{20}$$

The mixed-mean temperature out of burner B1, i.e., T_4 of Fig. 4, has a specified design point value of 3000° R. The total airflow required to achieve this specified temperature is obtained from an energy balance around burner B1. Thus, the total airflow (including bleed air to the topping loop) is given by the following equation:

$$W_a = \frac{(1 - X)(W_f)(\Delta H_{comb})}{(H_4 - H_3)} - W_f \tag{21}$$

An iterative procedure was used to solve equation (21). The procedure involved assuming a value of total airflow, W_a. This, in turn, fixes the composition of the flow mixture entering and leaving the burner. Then, the respective mixture enthalpies (H_3 and H_4) were computed from the relationship given by equation (7). This procedure was repeated, as required, until a solution of equation (21) was obtained.

(4) Heat Exchangers - The function of the heat exchangers in the topping loop is to reduce the temperature of the airflow entering the compressors. The air temperature at the outlet of each heat exchanger was assumed to have a design point value of 600° R. And each heat exchanger was assumed to have a design point pressure ratio of 0.99 (see Table I).

With reference to Fig. 4, the rate of heat transfer from the bleed airflow to the hydrogen flow is given by the following equations:

For heat exchanger HX-1,

$$Q_{HX-1} = W_{bleed} \int_{T_8}^{T_9} C_{p,a}\, dT \tag{22}$$

And for heat exchanger HX-2,

$$Q_{HX-2} = W_{bleed} \int_{T_{10}}^{T_{11}} C_{p,a}\, dT \tag{23}$$

The mixed-mean temperature of the hydrogen flow from heat exchangers HX-1 and HX-2 (i.e., T_{20}) was determined by equating the total heat transfer rate (Q_{HX-1} plus Q_{HX-2}) to the sensible heat gained by the hydrogen flow.

In a previously published report[10], an analysis was presented for the heat exchangers in the topping cycle engine. In that analysis, a particular compact heat exchanger core configuration was considered. Heat exchanger dimensions, surface

areas and weights were estimated for a reference topping cycle engine system which produces a net shaft power of 10,000 horsepower.

Weight Analysis

Engine system performance and engine system weight are key factors to consider in the comparison of aircraft propulsion systems. But some of the schemes proposed to improve aircraft engine system performance also result in increases in the system weight and complexity. In view of this, an engine system weight study was planned as a part of the overall topping cycle engine system analysis. The procedure used in this weight study is described below.

A digital computer program, called WATE-2[10], was used to estimate the weights of both the baseline and topping cycle engines. In order to provide a common basis by which these engine weights could be compared, a fixed shaft power output of 10,000 horsepower was assumed for each engine system.

The engine weight program (WATE-2) is designed to function in conjunction with a specific engine cycle analysis program, known as the NNEP[7]. As a prerequisite to operating the WATE-2 program, a digital simulation must be made for each engine system using the NNEP. Input to the NNEP includes engine thermodynamic data and component data along with logic and control data which describe the order, function, and arrangement of components in the engine system.

The thermodynamic output from the NNEP (which includes temperatures, pressures, flow rates, rotor speeds, shaft powers, etc.) is fed directly into the WATE-2 program. There, weights and dimensions are computed for each of the major components in the engine system. The total engine system weight is then determined by summing the weights of the components along with calculated weights of structural elements (such as frames, cases and support hardware) which are included in the engine system.

A separate analysis was made to estimate the weights and dimensions of the heat exchangers (HX-1 and HX-2) in the topping cycle engine. This was necessary because the heat exchanger analysis subprogram in WATE-2 is limited to compact heat exchangers in which both working fluids are air. The details of the heat exchanger analysis are presented in another report[10].

In the preceding paragraphs, we have given a brief description of the procedure used to estimate engine system weights. The accuracy of engine weight estimates from the WATE-2 program, as stated[9], is generally within ±10 percent. Results of the weight calculations for the baseline and topping cycle engines are presented and compared in the Results section of this report.

Results

Thermodynamic Performance

In this section, the thermodynamic performance of the topping cycle engine is presented and compared with that of a baseline (or reference) turboshaft engine which operates under the same cycle conditions. The engine system component characteristics and cycle conditions (design operating conditions) used in this study were introduced in the Thermodynamic Analysis section of this report.

Figure 6 depicts the performance of the topping cycle engine and baseline engine for the design operating conditions given in Table I. As illustrated in Fig. 6, the topping cycle engine has a significant performance advantage over the baseline engine. At the design conditions given in Table I, the thermal efficiency and brake specific fuel consumption of the topping cycle engine are about 12 percent better than that of the baseline engine.

Several of the design parameters in Table I were varied individually for the purpose of examining the topping cycle engine performance at other cycle conditions. The effects of these individual parametric changes on engine system performance are presented in the following paragraphs.

Effect of Compressor Pressure Ratio. Figure 7 shows the thermal efficiency and bsfc for the baseline and topping cycle engines against the pressure ratio of the main compressor (C1). Data in this figure were computed based on a constant design point burner outlet temperature of 3000° R. With reference to Fig. 7, the topping cycle engine shows a significant performance advantage over the baseline engine throughout the range of compressor pressure ratios shown. The relative difference in the curves of Fig. 7 ranges from about 12 percent at the design point pressure ratio (PR = 43.5) to about 20 percent at a pressure ratio of 15.0.

Effect of Burner Temperature. The design point value of burner temperature (Table I) was assumed to be 3000° R. Cycle calculations were made at other values of burner temperature for the purpose of determining the effect on engine performance. In Fig. 8, the baseline engine thermal efficiency and bsfc are presented against main compressor (C1) pressure ratio with burner temperature as a parameter. The trends shown in this figure are typical of a conventional turboshaft engine. That is, cycle performance improves with increasing burner temperature; and the optimum or near-optimum compressor pressure ratio (as shown by the dashed line in Fig. 8) increases with burner temperature.

A similar plot showing the effect of burner temperature on the topping cycle engine performance is depicted in Fig. 9. In the topping cycle engine, both burners, i.e., B1 and B2 of Fig. 4, are assumed to operate at the same constant temperature. A comparison of data in Figs. 8 and 9 indicates that the topping cycle engine performance is significantly better than the baseline

engine performance at all values of burner temperature. With the main compressor operating at the design point pressure ratio of 43.5, the relative difference in performance of these engines is approximately 12 percent for all constant values of burner temperature. At lower values of main compressor pressure ratio (e.g., near 15), the relative difference in performance of these engines is on the order of 15 to 20 percent for the range of operating temperatures shown in Figs. 8 and 9. Figure 9 also indicates that at the burner design point temperature of 3000° R, the optimum pressure ratio of the topping cycle engine is near the selected design point pressure ratio of 43.5, as given in Table I.

Effect of Precooling Compressor Air in Topping Loop. Precooling of the bleed air in the topping loop is accomplished with hydrogen-to-air heat exchangers (HX-1 and HX-2) as shown in Fig. 4. As stated in the section Description of Topping Cycle Engine, the purpose of precooling is to reduce the work requirements of compressors C2 and C3. The effect of precooling is shown in Fig. 10. In this figure, the thermal efficiency and bsfc of the topping cycle engine are presented against burner temperature for different values of compressor inlet temperature. As shown, the relative performance of the topping cycle engine increases with the level of precooling. At a burner temperature of 3000° R, i.e., at the design value, the relative performance gain from precooling is on the order of 1 percent for a change in compressor air inlet temperature of 100° R.

From the data in Fig. 10, it would appear that further improvements in performance could be obtained by precooling the bleed air to a temperature below the design point value of 600° R. However, there is a practical limit to the amount of precooling. At the design point operating conditions, the heat transfer rates in both of the heat exchangers are approximately equal and the design point effectiveness of each heat exchanger is in the neighborhood of 65 percent. Additional precooling would require a higher value of heat exchanger effectiveness which, in turn, would result in physically larger heat exchangers. Another point which should be considered in relation to the precooling is that a small amount of moisture (water vapor) is normally present in the ingested airflow, even at high altitude flight conditions. The likelihood of the entrained moisture condensing and freezing on the air-side surfaces of the heat exchangers would be expected to increase with the amount of precooling. To preclude this possibility and also to have the heat exchangers operate at a reasonable value of effectiveness, a minimum bleed air temperature of 600° R was assumed as a reasonable condition for this study.

Effect of Heat Exchanger Pressure Losses. At the design point, the pressure losses in the heat exchangers were assumed to be 1 percent of the inlet pressure. Thus, the design value for each of the individual ratios of pressure loss to inlet pressure (i.e., $\frac{(P_8 - P_9)}{P_8}$, $\frac{(P_{10} - P_{11})}{P_{10}}$, $\frac{(P_{18} - P_{19})}{P_{18}}$ and $\frac{(P_{16} - P_{17})}{P_{16}}$) was assumed equal to 0.01.

The sensitivity of the topping cycle engine performance to heat exchanger pressure losses is shown in Fig. 11. At the design point burner temperature of 3000° R, the data in Fig. 11 indicates that the relative change in performance is about 1 percent for each 5 percent change in heat exchanger pressure ratio (or 5 counts of pressure drop).

Effect of Compressor Pressure Ratio in Topping Loop. The effect of the topping loop compressor pressure ratio on engine performance is shown in Fig. 12. As indicated in this figure, cycle performance improves with increases in the topping loop compressor pressure ratio. There is, however, a practical upper limit to the compressor pressure ratio. At the design point, the pressure ratio across each compressor in the topping loop was equal to 6.10. (See Table I). This pressure ratio was chosen as a design value so as to limit the absolute pressure in the topping loop to a value of about 3000 psia.

From Fig. 12, it appears that additional improvements in performance may be realized by increasing the compressor pressure ratio above the design point value of 6.10. However, a relatively small increase in the compressor pressure ratio results in a large change in absolute pressure in the topping loop. For example, increasing the pressure ratio of each compressor in the topping loop from 6.10 to 7.0 results in a pressure increase of about 1000 psia in the topping loop.

Discussion of Topping Cycle Engine Performance

In the foregoing presentation, it was shown that the efficiency and/or bsfc of the topping cycle engine is about 12 percent better than that of a baseline turboshaft engine operating at the same cycle conditions. Before proceeding, it is important to note that a significant fraction of the net shaft power output of the topping cycle engine is generated by the auxiliary topping loop. At the design operating conditions, the topping loop delivers about 22 percent of the total shaft power output of this engine system. Thus, the efficiency with which this loop functions can have a significant effect on the overall performance of the topping cycle engine. In this section, we shall consider the individual factors which contribute to the overall performance gain associated with this engine system.

Precooling of Compressor Airflow in Topping Loop. The precooling of airflow upstream of each compressor in the topping loop reduces the work input to the compressors. Along with the compressor air precooling, the fuel is also preheated somewhat in this process. The combined effect of precooling the compressor airflow and preheating the fuel results in a cycle performance improvement of about 1 percent per 100° R change in the compressor inlet airflow temperature.

Utilization of Fuel as a Working Fluid. A significant net gain is realized from the use of

fuel as a working fluid in this cycle. The heated, unburned hydrogen fuel passing through the topping loop turbine generates a large fraction of the topping loop turbine power output. At the design conditions, only about 6 percent of the mass flow through the topping loop turbine is unburned hydrogen fuel. But, because hydrogen has a high specific heat (nearly 15 times that of air), the turbine work produced by the unburned hydrogen amounts to about 48 percent of the total work produced by this turbine. On the other hand, the pumping power required to boost the pressure of the cryogenic fuel (which is stored as a saturated liquid) is relatively small. At the design conditions, only about 2.5 percent of the power output of the topping loop turbine is used to drive the turbopump. Thus, in this cycle, the topping loop operates very efficiently. In terms of the overall performance gain associated with the topping cycle engine, approximately 80 percent of this gain can be attributed to the efficient way in which the fuel is used as a working fluid in the topping loop of this engine.

Engine System Weights

The results of the weight studies for the baseline engine and topping cycle engine are described below. Weight estimates obtained from the WATE-2 program and presented herein are based on a common shaft power output of 10,000 horsepower for each engine system. The procedure used in estimating engine system weights is described in the section Weight Analysis.

Baseline Engine. The calculated weights for the baseline engine are summarized in Table II. The baseline engine is actually a two-spool engine. And the turbomachinery weights listed in Table II include the individual high and low spool components. (The requirement of two spools is dictated by the relatively large overall pressure ratio of the engine.)

The compressor and turbine weights listed in Table II include the weights of the disc, blades, stators, connecting hardware, frame and case. But, as indicated in Table II, inlet and exhaust system weights are not included in the total engine system weight. The total weight of the baseline engine as estimated from the WATE-2 program is shown in Table II to be 850 lb_m.

Topping Cycle Engine. The calculated weights for the topping cycle engine are listed in Table III. The main gas turbine engine of this system also has two rotating spools.

The compressor and turbine weights in Table III include the same hardware items as described for the baseline engine. Gearbox weights and inlet and exhaust system weights are not included in the total topping cycle engine weight. The weights of the heat exchangers (HX-1 and HX-2) were obtained from a previously reported study[10].

Because of the relatively low mass flow rates in the topping loop, the compressors in this loop (C2 and C3) were assumed to be centrifugal machines. The total weight of the topping cycle engine as estimated from the WATE-2 program (and listed in Table III) is 865 lb_m. A comparison of the computed weights for the baseline and topping cycle engines indicates that they are nearly the same.

In comparing these engine weights, it is important to note that the specific power of the topping cycle engine is significantly greater than that of the baseline engine. (Specific power as used here is defined as the ratio of engine shaft power output to total engine airflow.) For a fixed value of shaft power output, the total airflow of the topping cycle engine was calculated to be about 28 percentage points less than that of the baseline engine. The lower airflow (or higher specific power) results in smaller and lighter-weight engine components. Thus, even though the topping cycle engine has an auxiliary flow loop which contains additional components, the estimated total weight of this engine system is comparable to that of the baseline turboshaft engine.

Summary of Results

The thermodynamic performance of the topping cycle engine was analyzed and compared with that of a reference turboshaft engine which operates under the same cycle conditions. For the cycle operating conditions selected, the performance of the topping cycle engine (i.e., the efficiency and/or specific fuel consumption) was determined to be about 12 percent better than that of a reference turboshaft engine.

The improved overall performance of this engine can be attributed to the fact that the auxiliary topping loop in this system operates at a high level of efficiency. In the auxiliary topping loop, cryogenic fuel (stored as a saturated liquid) is boosted to a high pressure by a turbopump. Because the fuel has a relatively small specific volume, the power expended in pumping the fuel is also relatively small, even for the large pressure change. The high pressure-low temperature fuel is also used to precool the bleed airflow in this loop before compression. This, in turn, reduces the work required to compress the bleed airflow. Finally, the high pressure fuel is heated and a portion of it is then expanded through an auxiliary power turbine to produce additional shaft power. The combination of these processes result in a significant improvement in the overall performance of this engine.

The results of the weight comparison between the topping cycle engine and the baseline turboshaft engine indicate that these engines have nearly the same weight. The weight comparison was based on a common shaft power output of 10,000 horsepower for each engine.

It is concluded, therefore, that the topping cycle engine has significantly better thermodynamic performance than that of the baseline turboshaft engine. And the estimated weight of the topping cycle engine is comparable to that of the baseline turboshaft engine.

References

1. "The Global 2000 Report to the President: Entering the Twenty-First Century," Council

on Environmental Quality, Washington, D.C., 1980.

3. Witcofski, R. D., "Comparison of Alternate Fuels for Aircraft," NASA TM-80155, 1979.

3. Brewer, G. D., and Morris, R. E, "Study of LH_2 - Fueled Subsonic Passenger Transport Aircraft," Lockheed-California Co., Burbank, CA, LR-27446, Jan. 1976. (NASA CR-144935.)

4. Whitlow, J. B., Jr., Weber, R. J., and Civinskas, K.C., "Preliminary Appraisal of Hydrogen and Methane Fuel in a Mach 2.7 Supersonic Transport," NASA TMX-68222, 1973.

5. Miller, B. A., "Analysis of Several Methane - Fueled Engine Cycles for Mach 3.0 Flight," NASA TND-4699, 1968.

6. Hendricks, R. C., Baron, A. K., and Peller, I. C., "GASP - A Computer Code for Calculating the Thermodynamic and Transport Properties for Ten Fluids: Parahydrogen, Helium, Neon, Methane, Nitrogen, Carbon Monoxide, Oxygen, Fluorine, Argon, and Carbon Dioxide," NASA TND-7808, 1975.

7. Fishbach, L. H., and Caddy, M. J., "NNEP - The Navy-NASA Engine Program," NASA TMX-71857, 1975

8. Hendricks, R. C., Peller, I. C., and Baron, A. K., "WASP - A Flexible Fortran IV Computer Code for Calculating Water and Steam Properties," NASA TND-7391, 1973.

9. Onat, E., and Klees, G. W., "A Method to Estimate Weight and Dimensions of Large and Small Gas Turbine Engines," NASA CR-159481, 1979.

10. Turney, G. E., and Fishbach, L. H., "Analysis of a Topping Cycle Aircraft Gas Turbine Engine System Which Uses Cryogenic Fuel," NASA TP-2219, 1983.

TABLE I. - DESIGN POINT OPERATING CONDITIONS AND COMPONENT CHARACTERISTICS FOR BASELINE ENGINE AND TOPPING CYCLE ENGINE AT FLIGHT CONDITIONS OF MACH 0.8, 35,000 FEET

	Baseline engine	Topping cycle engine
Component or cycle parameter:		
Inlet recovery, P_1/P_0	1.0	1.0
Burner temperatures:		
Burner-B1, T_4 °R	3000	3000
Burner-B2, T_{14} °R	----	3000
Efficiencies:		
Hydrogen pump-P	.60	.60
Main compressor-C1	.88	.88
Compressor-C2	----	.88
Compressor-C3	----	.88
Main turbine-T1	.86	.86
Turbine-T2	----	.86
Burner-B1	1.0	1.0
Burner-B2	1.0	1.0
Component pressure ratios:		
Main compressor-C1, P_2/P_1	43.5	43.5
Compressor-C2, P_{10}/P_9	----	6.1
Compressor-C3, P_{12}/P_{11}	----	6.1
Burner-B1, P_4/P_3	.95	.95
Burner-B2, P_{14}/P_{13}	----	.95
Fuel storage (sat. liquid):		
Pressure, P_6, psia	14.696	14.696
Temperature, T_6, °R	36.608	36.608
Bleed air pressure, P_8, psia	----	81.0
Compressor-C2 inlet temp., T_9, °R	----	600
Compressor-C3 inlet temp., T_{11}, °R	----	600
Turbine-T1 discharge press., P_5, psia	5.27	5.27
Heat exchanger pressure ratios:		
Air side, P_9/P_8 and P_{11}/P_{10}	----	.99
Hydrogen side, P_{17}/P_{16} and P_{19}/P_{18}	----	.99

TABLE II. - SUMMARY OF COMPONENT WEIGHTS AND ENGINE SYSTEM WEIGHT FOR ADVANCED 10,000 HORSEPOWER BASELINE TURBOSHAFT ENGINE

Component	Weight, lb_m
Compressor (C1):	
LPC	347
HPC	101
Burner (B1)	81
Turbine (T1):	
HPT	69
LPT	125
Shafting	28
Controls and accessories	99
Total engine	850

TABLE III. - SUMMARY OF COMPONENT WEIGHTS AND ENGINE SYSTEM WEIGHT FOR 10,000 HORSEPOWER TOPPING CYCLE ENGINE

Component	Weight, lb_m
Main gas turbine engine:	
Compressor (C1):	
LPC	271
HPC	82
Burner (B1)	62
Turbine (T1):	
HPT	52
LPT	100
Shafting	22
Controls and accessories	75
Main gas turbine engine	664
Topping loop:	
Compressors (C2)	40
Compressors (C3)	20
Burner (B2)	22
Turbine (T2)	57
Heat exchanger (HX-1)	9
Heat exchanger (HX-2)	20
Shafting	11
Controls and accessories	22
Topping loop	201
Total Engine	865

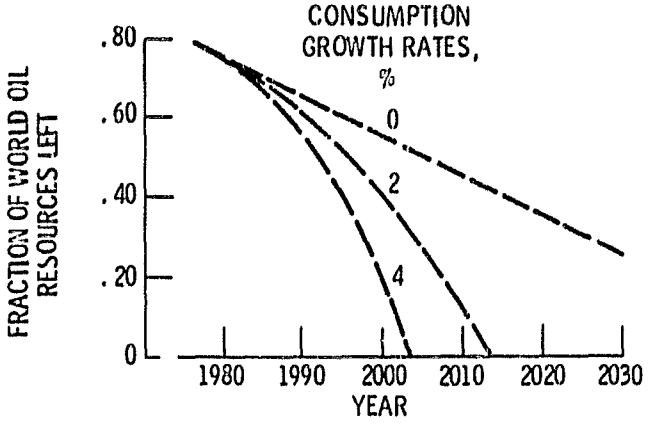

Figure 1. - Fraction of world oil resources left against time for consumption growth rates of 0, 2, and 4 percent.

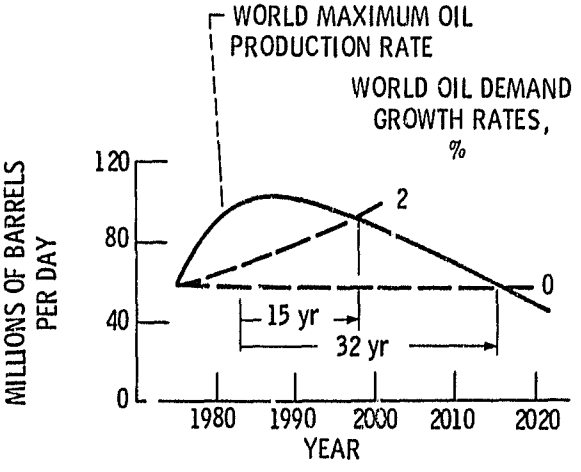

Figure 2. - Estimates of world maximum oil production and demand for growth rates of 0 and 2 percent.

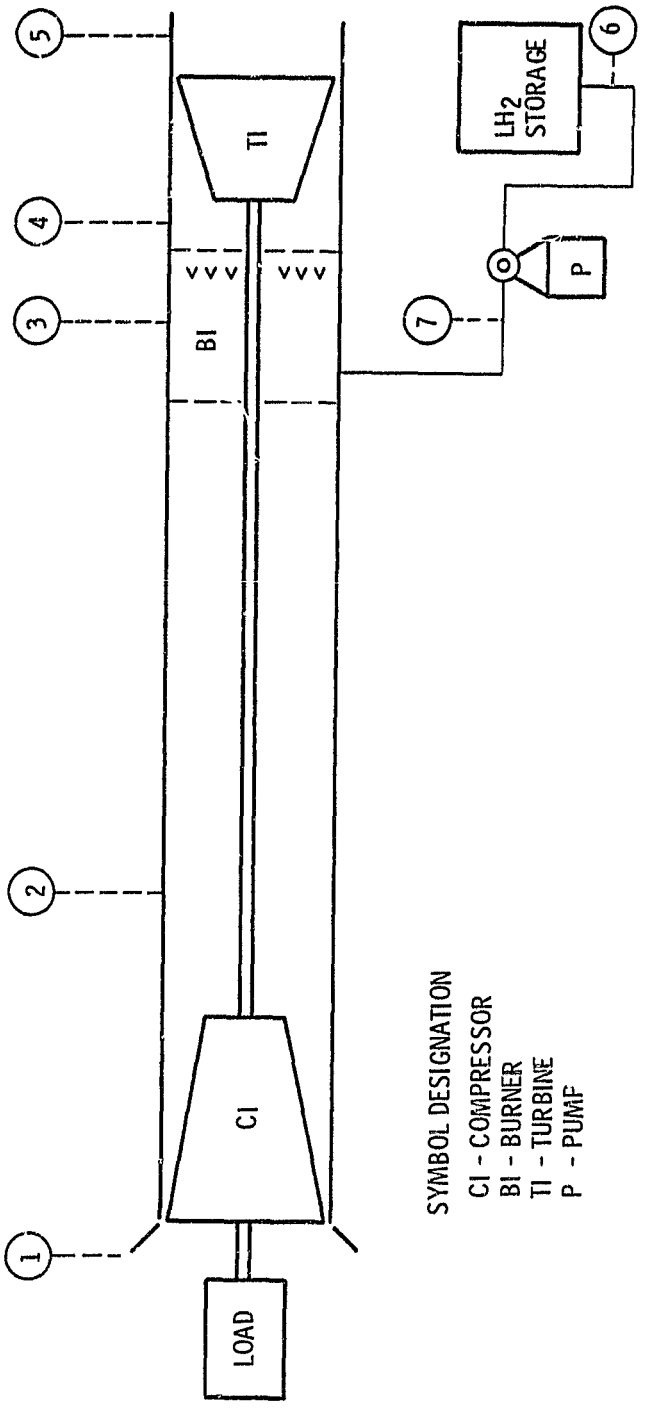

Figure 3. - Baseline hydrogen-fueled turboshaft engine.

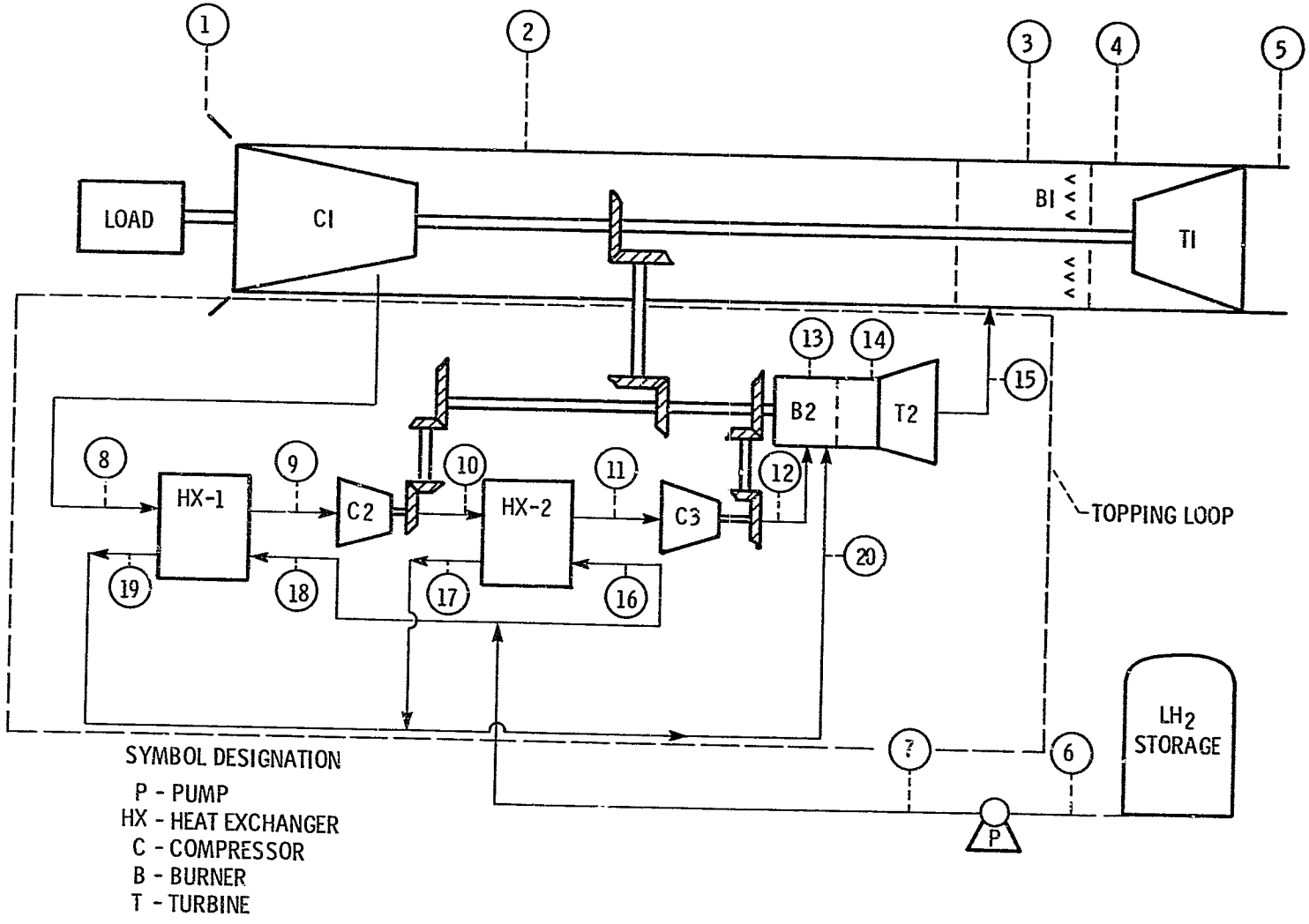

Figure 4. - Simplified sketch of hydrogen - fueled topping cycle engine.

SYSTEM PRESSURES	
LOCATION	PRESSURE, psia
1	5.27
2	229.0
3	229.0
4	217.55
5	5.27
8	80.91
9	80.10
10	487.73
11	482.86
12	2940.11
14	2793.11

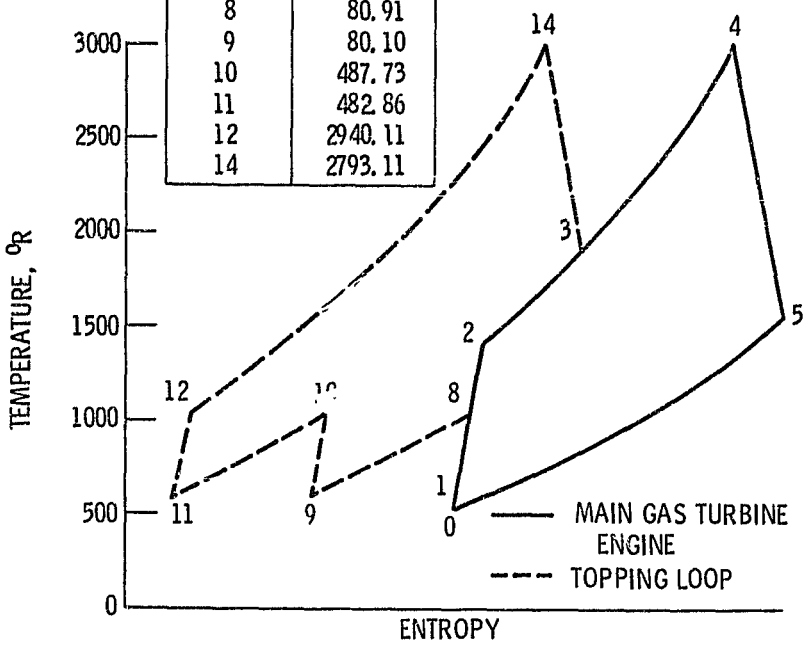

Figure 5. - Temperature-entropy illustration for topping cycle engine operating at design point conditions.

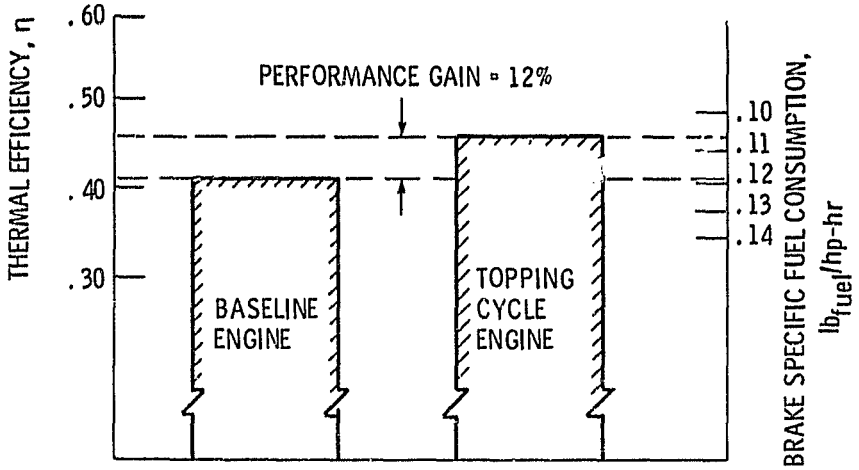

Figure 6. - Comparison of baseline engine and topping cycle engine performance at design point operating conditions - Mach 0.8, 35 000 ft.

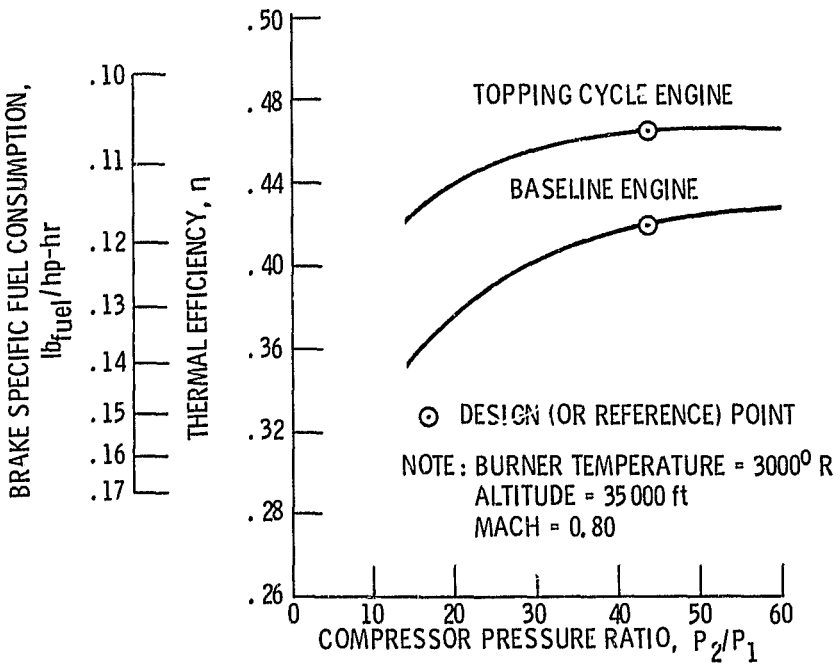

Figure 7. - Thermal efficiency and bsfc against compressor pressure ratio of baseline and topping cycle engines with constant burner temperature of 3000° R.

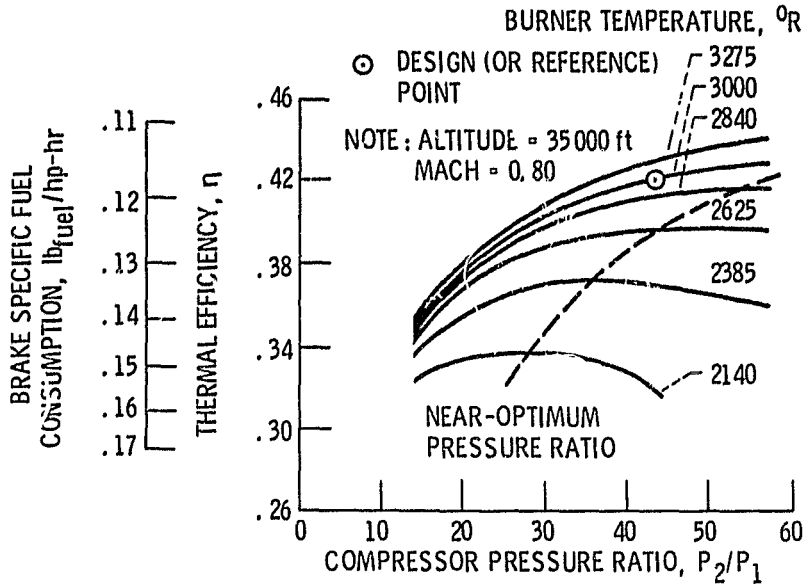

Figure 8. - Baseline engine thermal efficiency and bsfc against compressor pressure ratio with burner temperature as a parameter.

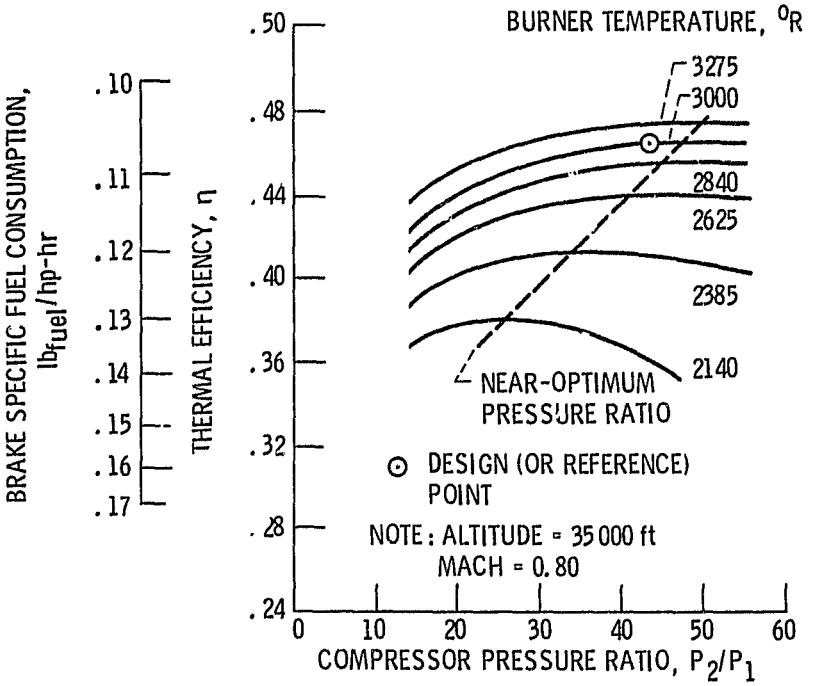

Figure 9. - Topping cycle engine thermal efficiency and bsfc against compressor pressure ratio with burner temperature as a parameter.

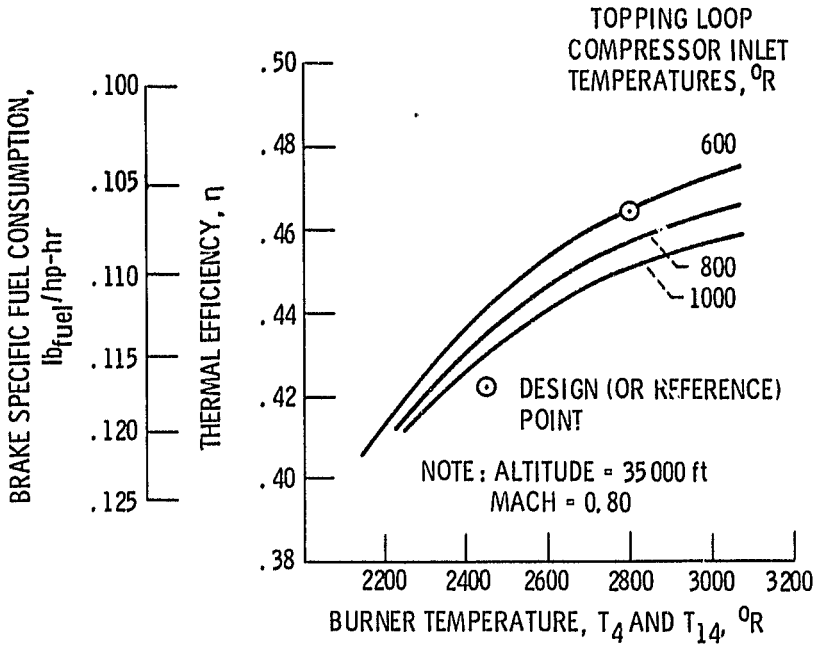

Figure 10. - Topping cycle engine thermal efficiency and bsfc against burner temperature with topping loop compressor inlet temperatures as a parameter.

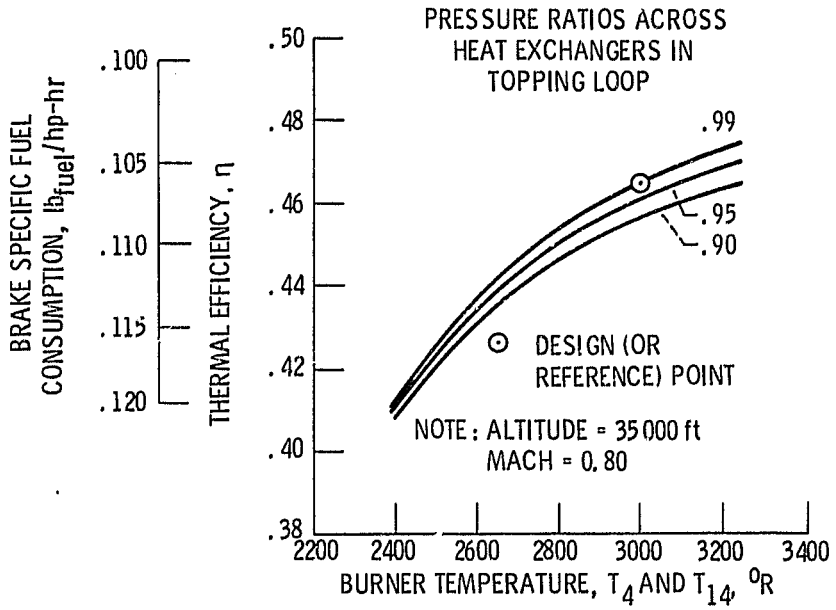

Figure 11. - Topping cycle engine thermal efficiency and bsfc against burner temperature with heat exchanger pressure ratio as a parameter.